

Exploring the onset of quasifission by measurement of mass distribution in $^{19}\text{F}+^{184}\text{W}$

S. Nath^{1,2,a}, K.S. Golda¹, A. Jhingan¹, J. Gehlot¹, E. Prasad³, Sunil Kalkal⁴, M.B. Naik⁵, P. Sugathan¹, N. Madhavan¹, and P.V. Madhusudhana Rao²

¹ Inter University Accelerator Centre, Aruna Asaf Ali Marg, Post Box 10502, New Delhi 110067, India

² Department of Nuclear Physics, Andhra University, Visakhapatnam 503003, India

³ Department of Physics, Calicut University, Calicut 673635, India

⁴ Department of Physics and Astrophysics, Delhi University, Delhi 110007, India

⁵ Department of Physics, Karnatak University, Dharwad 580003, India

Abstract. Fission fragment mass distributions for $^{19}\text{F}+^{184}\text{W}$ have been measured at beam energies in the range of 85 - 125 MeV. Analysis of mass distribution width indicates that the system proceeds towards the formation of compound nucleus. No signature of quasifission is observed in this reaction. These results strengthen the conclusions of our earlier works revealing the stabilizing effect of the $Z = 82$ shell closure against fission.

1 Introduction

Extending the limit of the periodic table of elements has been an area of intense theoretical and experimental investigation for the last few decades [1, 2]. Quasifission [3–7], in which the composite system formed after capture of projectile and target disintegrates before forming a compound nucleus (CN), is a major roadblock towards that goal. There have been general agreement that entrance channel mass asymmetry η ($=\frac{|A_p-A_t|}{A_p+A_t}$, A_p and A_t are projectile and target masses, respectively), charge product of projectile and target ($Z_p Z_t$), mean fissility of the CN (χ_m), static deformation and relative orientation of the reaction partners affect quasifission probability (P_{QF}). Experimental signatures of quasifission include anomalous behaviour of fission fragment (FF) angular anisotropy, FF mass angle correlation, broadened FF mass distribution and reduction of evaporation residue (ER) cross section (σ_{ER}). This qualitative understanding of quasifission evolved from many experiments using varied probes, carried out over the years.

A few recent measurements, though, have brought out several discrepancies in our understanding of quasifission. Evidence of quasifission in the system $^{19}\text{F}+^{197}\text{Au}$ was found by measurement of σ_{ER} [8]. But the FF angular distribution for the same system could be explained by CN fission only [9]. Appannababu et al. [10] reported absence of quasifission in the system $^{27}\text{Al}+^{186}\text{W}$ by measuring FF mass angle correlation and mass ratio distribution. However, Prasad et al. [11] found evidence of quasifission in the more asymmetric system $^{24}\text{Mg}+^{186}\text{W}$ by similar measurement. Another notable system is $^{16}\text{O}+^{238}\text{U}$ [12], in which onset of quasifission was observed by FF mass distribution and angular anisotropy measurement. But measured

precission neutron multiplicity and σ_{ER} for the same system did not show any departure from standard statistical model predictions. Thus, the knowledge about the relative sensitivity of different probes to study quasifission and a comprehensive and quantitative understanding of the process are still elusive. Therefore, it is imperative to pursue a systematic study on the factors affecting quasifission.

Also, precise knowledge of the CN formation probability ($P_{CN} = 1 - P_{QF}$) is important in interpreting ER yields in many reactions. We had earlier measured ER excitation function [13] and ER-gated CN angular momentum distribution [14] for the system $^{19}\text{F}+^{184}\text{W}$. We had compared σ_{ER} for the systems $^{19}\text{F}+^{175}\text{Lu}$ [15], $^{19}\text{F}+^{181}\text{Ta}$ [16, 17], $^{19}\text{F}+^{184}\text{W}$ [13] and $^{19}\text{F}+^{188}\text{Os}$ [18] leading to the CN $^{194}_{80}\text{Hg}$, $^{200}_{82}\text{Pb}$, $^{203}_{83}\text{Bi}$ and $^{207}_{85}\text{At}$, respectively. We had performed statistical model calculation and extracted the best-fit value of the fission barrier ($B_f(0)$) for each system. The fitted value of $B_f(0)$ had been observed to be substantially enhanced for the system with $Z = 82$ in the CN ($^{200}_{82}\text{Pb}$), compared to the other neighbouring systems. We had interpreted the enhancement as being caused by the shell closure effect at $Z = 82$, which provided the additional stability against fission for ^{200}Pb . We had also compared the angular momentum distributions for the formation of ERs for the systems $^{19}\text{F}+^{175}\text{Lu}$ and $^{19}\text{F}+^{184}\text{W}$ at similar $\frac{E_{c.m.}}{V_{Coul.}}$, where $V_{Coul.}$ is the Coulomb barrier. We had observed the higher angular momenta to be somewhat depleted in the heavier system compared to the lighter system, thereby bringing out the stabilizing effect of the $Z = 82$ shell against fission.

We report here measurement of FF mass distribution, in our attempt to study the onset of quasifission, if any, in the system $^{19}\text{F}+^{184}\text{W}$. Details of the experiment are described in Section 2, results are presented in Section 3, followed by a discussion in Section 4.

^a e-mail: subir@iuac.res.in

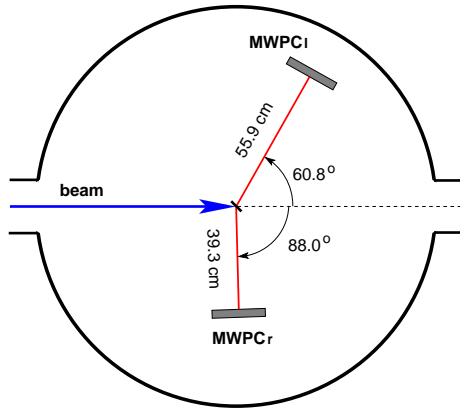


Fig. 1. Schematic of the experimental setup used for FF mass distribution.

2 The experiment

The experiment was performed at the 15UD Pelletron accelerator facility of the Inter University Accelerator Centre (IUAC), New Delhi. A pulsed beam of ^{19}F with 250 ns pulse separation and ~ 1 ns pulse width was bombarded onto a $210 \mu\text{g}/\text{cm}^2$ ^{184}W target [19] on a $110 \mu\text{g}/\text{cm}^2$ carbon backing. Measurements were carried out at laboratory beam energies of 84.8, 89.8, 94.8, 99.8, 104.8, 109.8, 114.8, 119.8 and 124.8 MeV (corrected for the energy loss in the half thickness of the target). A schematic of the experimental set up is shown in Fig. 1. Two multi-wire proportional counters (MWPCs) [20] of active area $20 \times 10 \text{ cm}^2$ were used to detect the FFs in coincidence. The MWPCs were mounted on the two rotatable arms, at folding angles, inside a large scattering chamber: the forward detector (MWPC_f) centered at polar angle (θ) = 60.8° (azimuthal angle, $\phi = 90^\circ$) and the backward detector (MWPC_r) centered at $\theta = 88^\circ$ ($\phi = 270^\circ$). The nearest distance to MWPC_f from the target was 55.9 cm and that to MWPC_r was 39.3 cm. The target was mounted with the carbon backing oriented downstream. It was tilted at 45° with respect to the beam direction and about a vertical axis to minimize energy loss of FFs in the target and to avoid shadowing of the detectors by the target ladder. The MWPCs were operated with isobutane gas at a pressure of 3.0 mbar and provided very good position and timing resolution. Two silicon detectors were mounted at $\pm 10^\circ$ with respect to the beam direction to monitor beam current and to position the beam at the centre of the target. Timing from one of these monitor detectors was fed to a time-to-amplitude converter (TAC) as the start signal while the radio frequency (RF) pulse, used for beam pulsing, provided the stop. The resulting TAC spectrum, showing the time structure of the beam, was closely monitored throughout the experiment. Position information of the FFs was obtained from the delay-line readout of the wire planes. The fast timing signals from the anodes of the two MWPCs were used to obtain the FF time of flight (TOF) with respect to the beam pulse. A fast coincidence between any of the anode signals and the RF pulse was used as the master trigger for data acquisition.

Analysis of data has been performed using CANDLE [21].

3 Data analysis and results

The first step in data analysis is the unambiguous identification and separation of coincident fission events from other events. We plot the difference in timing signals ($\Delta t = t_l - t_r$) versus the sum of the energy loss signals ($\Delta E_l + \Delta E_r$) from the two MWPCs in Fig. 2. We observe three major group of events, marked by numbers in the figure. The first group represented the events in which two complimentary FFs were detected in the two MWPCs, kept at the folding angles. For determining FF mass distribution, only these events were analyzed further. The coincident fission events can also be identified by time correlation alone, as shown in Fig. 3.

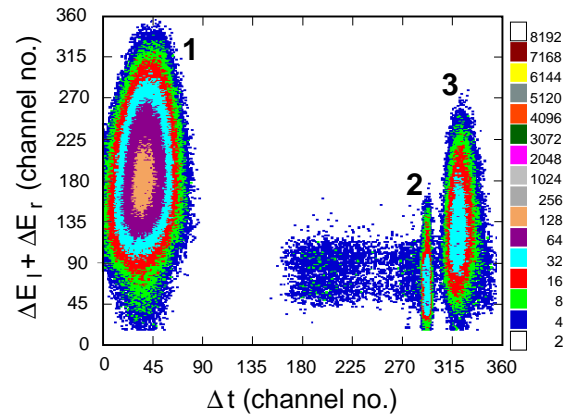


Fig. 2. Identification of different group of events based on the timing and energy loss signals from the two MWPCs at the laboratory energy 99.8 MeV. The group marked 1 represents events when two complimentary FFs were detected at the two detectors simultaneously. The group marked 2 denotes the elastic events detected only by MWPC_f. The group marked 3 indicates the events in which only one of the fragments was detected by MWPC_f.

The time difference method [22] has been employed to extract FF mass distribution. It is well established that the time difference method is valid only when the target used in the reaction is nonfissile and therefore transfer-induced fission is negligibly small. This condition is satisfied in the present reaction. Binary division of the composite system into two FFs is expected after full momentum transfer. Therefore, application of the time difference method is justified in this case.

Each event on the active area of the detectors has been transformed to give the scattering angles with respect to the beam axis. The masses of the FFs have been reconstructed by using the scattering angles and flight time difference of the complimentary FFs using the following set of equations [22]:

$$m_1 = \frac{(t_1 - t_2) + \delta t_0 + m_{CN} \frac{d_2}{p_2}}{\frac{d_1}{p_1} + \frac{d_2}{p_2}}, \quad (1)$$

$$m_2 = m_{CN} - m_1, \quad (2)$$

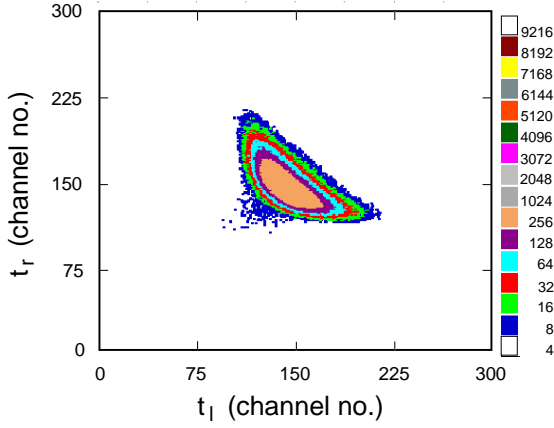


Fig. 3. Identification of simultaneously detected FFs (events marked **1** in Fig. 2) at the laboratory energy 99.8 MeV by time correlation.

$$p_1 = \frac{m_{CN} V_{CN}}{\cos\theta_1 + \sin\theta_1 \cot\theta_2}, \quad (3)$$

$$p_2 = \frac{p_1 \sin\theta_1}{\sin\theta_2}, \quad (4)$$

where m_1, m_2 are the masses of FFs; t_1 and t_2 are the flight times of the fragments for the flight paths d_1 and d_2 ; p_1 and p_2 are the linear momenta of the fragments in laboratory frame; m_{CN} and V_{CN} are the mass and velocity of the CN. The electronic delay between the two timing signals δt_0 has been determined precisely at each beam energy assuming the condition of identity of the measured mass distributions in the two detectors and Viola systematics [23] for fission fragment total kinetic energy.

The resulting FF mass distributions are shown in Fig. 4, along with Gaussian fits.

4 Discussion

We observe that the measured mass distribution spectra (Fig. 4) are well described by Gaussians at all energy points. The variation of the standard deviation (σ_m) of the fitted Gaussian to the experimental FF mass distribution as a function of centre of mass energy ($E_{c.m.}$) is shown in Fig. 5. We do not observe any anomalous increase of the width in the energy range studied, which is often interpreted as the signature of deviation from CN behaviour [24]. Therefore, we conclude that the present system proceeds towards the formation of CN after capture and quasifission is not observed.

We also study the variation of the variance of FF mass distribution (σ_m^2) with the temperature of the fissioning CN,

$$T = \sqrt{\frac{E^*}{a}}, \quad (5)$$

$$E^* = E_{c.m.} + Q - B_f(l) - E_{rot}(l) - E_n^{pre}. \quad (6)$$

Here E^* is the excitation energy at the saddle point, $a = \frac{A_{CN}}{10}$ is the level density parameter, A_{CN} is the CN mass. Q

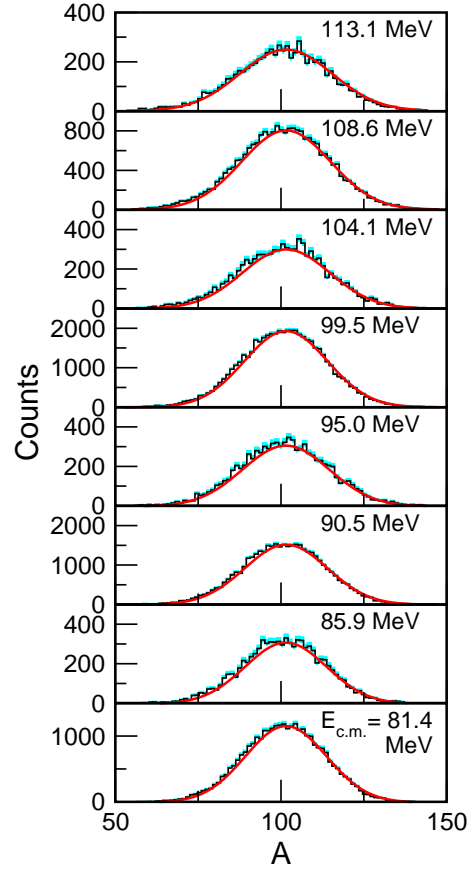


Fig. 4. Measured FF mass distribution (shown as histogram) for the system $^{19}\text{F}+^{184}\text{W}$. The statistical errors are shown by shades. The continuous line is the Gaussian fit at each energy. FF mass distribution at the lowest beam energy (84.8 MeV) is not shown because of insufficient statistics.

is the Q -value for CN formation. $B_f(l)$, $E_{rot}(l)$ and E_n^{pre} are l -dependent fission barrier, l -dependent rotational energy and the reduction in excitation energy of the CN by neutron evaporation, respectively. These three quantities have been calculated in a way similar to that described in Ref. [11]. Fig. 6 reveals a linear variation of σ_m^2 with temperature,

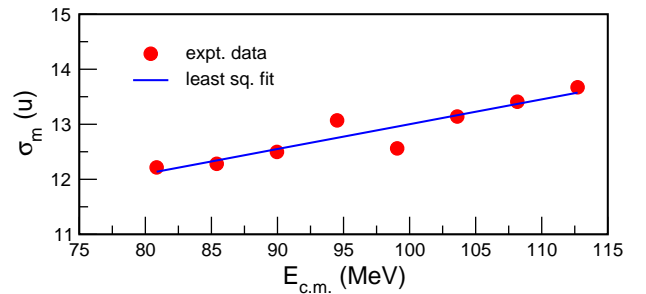


Fig. 5. The standard deviation of the Gaussian fit to the FF mass distribution for the system $^{19}\text{F}+^{184}\text{W}$ as a function of $E_{c.m.}$. The straight line is the least square fit to data points. Errors are less than the symbol size.

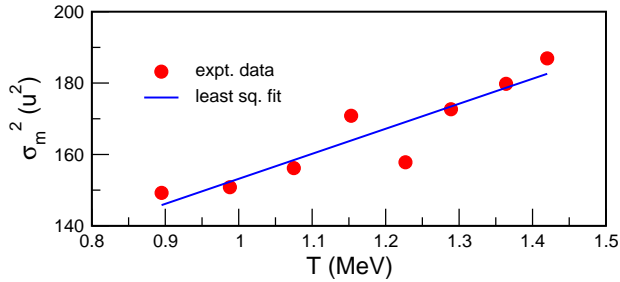


Fig. 6. The variance of the Gaussian fit to the FF mass distribution for the system $^{19}\text{F}+^{184}\text{W}$ as a function of saddle point temperature. The straight line is the least square fit to data points. Errors are less than the symbol size.

confirming that CN fission is the dominant channel.

Acknowledgments

We thank the Pelletron staff of IUAC for providing pulsed beam of excellent quality and Dr. A. Roy for useful discussions.

References

1. Yuri Oganessian, *J. Phys. G* **34**, R165 (2007).
2. S. Hofmann and G. Münzenberg, *Rev. Mod. Phys.* **72**, 733 (2000).
3. W.J. Swiatecki, *Phys. Scr.* **24**, 113 (1981).
4. S. Bjørnholm and W.J. Swiatecki, *Nucl. Phys. A* **391**, 471 (1982).
5. B.B. Back, *Phys. Rev. C* **31**, 2104 (1985).
6. J. Töke, R. Bock, G.X. Dai, A. Gobbi, S. Gralla, K.D. Hildenbrand, J. Kuzminski, W.F.J. Müller, A. Olmi, H. Stelzer, B.B. Back and S. Bjørnholm, *Nucl. Phys. A* **440**, 327 (1985).
7. J.P. Blocki, H. Feldmeier and W.J. Swiatecki, *Nucl. Phys. A* **459**, 145 (1986).
8. A.C. Berriman, D.J. Hinde, M. Dasgupta, C.R. Morton, R.D. Butt and J.O. Newton, *Nature (London)* **413**, 144 (2001).
9. R. Tripathi, K. Sudarshan, S. Sodaye, A.V.R. Reddy, K. Mahata and A. Goswami, *Phys. Rev. C* **71**, 044616 (2005).
10. S. Appannababu, S. Mukherjee, B.K. Nayak, R.G. Thomas, P. Sugathan, A. Jhingan, E. Prasad, D. Negi, N.N. Deshmukh, P.K. Rath, N.L. Singh and R.K. Choudhury, *Phys. Rev. C* **83**, 034605 (2011).
11. E. Prasad, K.M. Varier, R.G. Thomas, P. Sugathan, A. Jhingan, N. Madhavan, B.R.S. Babu, Rohit Sandal, Sunil Kalkal, S. Appannababu, J. Gehlot, K.S. Golda, S. Nath, A.M. Vinodkumar, B.P. Ajith Kumar, B.V. John, Gayatri Mohanto, M.M. Musthafa, R. Singh, A.K. Sinha and S. Kailas, *Phys. Rev. C* **81**, 054608 (2010).
12. K. Banerjee, T.K. Ghosh, S. Bhattacharya, C. Bhattacharya, S. Kundu, T.K. Rana, G. Mukherjee, J.K. Meena, J. Sadhukhan, S. Pal, P. Bhattacharya, K.S. Golda, P. Sugathan and R.P. Singh, *Phys. Rev. C* **83**, 024605 (2011).
13. S. Nath, P.V. Madhusudhana Rao, Santanu Pal, J. Gehlot, E. Prasad, Gayatri Mohanto, Sunil Kalkal, Jhiling Sadhukhan, P.D. Shidling, K.S. Golda, A. Jhingan, N. Madhavan, S. Muralithar and A.K. Sinha, *Phys. Rev. C* **81**, 064601 (2010).
14. S. Nath, J. Gehlot, E. Prasad, Jhiling Sadhukhan, P.D. Shidling, N. Madhavan, S. Muralithar, K.S. Golda, A. Jhingan, T. Varughese, P.V. Madhusudhana Rao, A.K. Sinha and Santanu Pal, *Nucl. Phys. A* **850**, 22 (2011).
15. S.K. Hui, C.R. Bhuinya, A.K. Ganguly, N. Madhavan, J.J. Das, P. Sugathan, D.O. Kataria, S. Muralithar, Lagy T. Baby, Vandana Tripathi, Akhil Jhingan, A.K. Sinha, P.V. Madhusudhana Rao, N.V.S.V. Prasad, A.M. Vinodkumar, R. Singh, M. Thoennessen and G. Gervais, *Phys. Rev. C* **62**, 054604 (2000).
16. A.L. Caraley, B.P. Henry, J.P. Lestone and R. Vandenbosch, *Phys. Rev. C* **62**, 054612 (2000).
17. D.J. Hinde, J.R. Leigh, J.O. Newton, W. Galster and S. Sie, *Nucl. Phys. A* **385**, 109 (1982).
18. K. Mahata, S. Kailas, A. Shrivastava, A. Chatterjee, A. Navin, P. Singh, S. Santra and B.S. Tomar, *Nucl. Phys. A* **720**, 209 (2003).
19. P.D. Shidling, S.R. Abhilash, D. Kabiraj, N. Madhavan, *Nucl. Instr. Meth. A* **590**, 79 (2008).
20. A. Jhingan, P. Sugathan, K.S. Golda, R.P. Singh, T. Varughese, Hardev Singh, B.R. Behera and S.K. Mandal, *Rev. Sci. Instrum.* **80**, 123502 (2009).
21. E. T. Subramaniam, B. P. Ajith Kumar, and R. K. Bhowmik, Collection and Analysis of Nuclear Data using Linux nEtnetwork (unpublished).
22. R.K. Choudhury, A. Saxena, A. Chatterjee, D.V. Shetty, S.S. Kapoor, M. Cinausero, L. Corradi, E. Farnea, E. Fioretto, A. Gadea, D. Napoli, G. Prete, A.M. Stefanini, D. Bazzaco, S. Beghini, D. Fabris, G. Montagnoli, G. Nebbia, C. Rossi-Alvarez, F. Scarlasara, C. Ur and G. Viesti, *Phys. Rev. C* **60**, 054609 (1999).
23. V.E. Viola, K. Kwiatkowski and M. Walker, *Phys. Rev. C* **31**, 1550 (1985).
24. T.K. Ghosh, S. Pal, K.S. Golda and P. Bhattacharya, *Phys. Lett. B* **627**, 26 (2005).